THE ASTROPHYSICAL JOURNAL, 388:383–391, 1992 April 1

DUST WITHIN GLOBULAR CLUSTERS: A LARGE BUBBLE IN NGC 6624?

JUAN C. FORTE[1,2]
Instituto de Astronomía y Física del Espacio, C.C. 67, Succ. 28, 1428 Buenos Aires, Argentina
SERGIO A. CELLONE AND MARIANO MÉNDEZ[1]
Facultad de Ciencias Astronómicas y Geofísicas de la Universidad Nacional de La Plata, Paseo del Bosgue, 1900 La Plata, Argentina
AND
E. IRENE VEGA
Complejo Astronómico El Leoncito, Santa Fé 198 Oeste, 5400 San Juan, Argentina
Received 1990 October 19; accepted 1991 September 25

ABSTRACT

An analysis of dark patches, based on multicolor CCD frames, and polarimetry of stars in the field of the globular cluster NGC 6624 are presented. The apparent extinctions in a number of dark patches reveal a nongray behavior with wavelength. The fitting of a given extinction law indicates minimum intrinsic visual extinctions ranging from 0.20 to 0.30 mag. These results are consistent with photometric measurements made in annular segments and with differential reddening effects in the C-M diagram, suggesting the existence of a large-scale dust feature associated with the cluster. The overall appearance of the distribution of the dark patches is reminiscent of a bubble-like geometry not centered at the cluster nucleus and with a 50″ radius. The apparent center of this structure is located at some 9″ from the position of the X-ray burster 1820−30.

Subject headings: dust, extinction — globular clusters: individual (NGC 6624) — polarization

1. INTRODUCTION

The nature of dark patches in globular clusters has been a controversial subject over the years. Some recent arguments based on multicolor CCD observations (Forte & Méndez 1987, hereafter FM; Méndez, Forte, & Orsatti 1989) and polarimetry (Forte & Méndez 1989) seem consistent with the dust hypothesis.

On the other side, alternative interpretations (Aurière & Leroy 1990) suggest that the same arguments, although not inconsistent, are not conclusive. This work presents an analysis of NGC 6624 where previous results suggested the existence of a large-scale structure instead of the presence of a few isolated dark patches (FM). This is not a completely uncommon situation in globular clusters and the case of M13, described by Lord Rosse (1861), is a good example of a similar feature.

Besides the historical aspects of the topic, it is clear that the existence (or lack of it) of dust is closely connected with the longstanding problem of the apparent absence of gas within globular clusters, and the role of mass ejection from red giants or from pre–planetary nebula objects. Feasible mechanisms have been proposed to explain this situation (Scott & Durisen 1978, VandenBerg 1978), but an unambiguous solution to the problem is still lacking.

The core of the analysis in this work is, as in previous papers, the behavior of the apparent extinctions of the dark patches at different wavelengths. These extinctions are measured with respect to a reference level defined by a modal background at each wavelength. The main assumption which requires an independent check, is that the foreground extinction along the line of sight to the cluster is uniform within the area under study.

In principle, the dark patches statistics will be dominated by random fluctuations in the distribution of the stars that, if the reference modal level is properly set, will show a gray extinction behavior. Color variations are certainly expected if (1) the window used to measure the extinction is too small and introduces strong Poissonian sampling noise or (2) the reference level is not defined adequately (as in the example given by Aurière & Leroy 1990).

On the other hand, dust cloud candidates will be selected if the multicolor extinctions show a slope, with wavelength, which is significantly different from zero and consistent with the expectations from a given selective extinction law.

The interpretation of the observed apparent extinctions in terms of a cloud with a given optical depth requires a number of assumptions discussed in the following paragraphs. We also looked for independent observations that could be compared with the results obtained from that kind of analysis, namely, integrated photometry on the original images and the appearance of the C-M diagram of the cluster.

2. OBSERVATIONS AND DATA HANDLING

2.1. *Direct Images*

CCD observations in the UBV-RI_{KC} bands were obtained with the 0.9 m telescope at CTIO and are listed in Table 1. The resulting scale was 0.″49 per pixel. Dome flats were obtained each night and confronted with deep sky frames. These comparisons suggested that the resulting flattening is uncertain at 2% level.

The ultraviolet images, taken with the TI chip, have slightly different centers in order to decrease the effect of flat-fielding uncertainties on the average extinctions.

The link to the standard system was made through the transformation equations given in FM for the $BVRI$ bands. Alternatively, the U images were calibrated using concentric aperture photometry and the $U-B$ colors given by van den Bergh (1977).

[1] Visiting Astronomer, Cerro Tololo Inter-American Observatory, operated by AURA under contract with the National Science Foundation.
[2] Astrónomo Visitante, Complejo Astronómico El Leoncito San Juan, Argentina.

TABLE 1

CCD LOGBOOK

Filter	Date	Exposure (s)	Chip
U	1987 Sep 14	450 (×3)	TI
B	1985 Aug 10	180	RCA
V	1985 Aug 10	150	RCA
R	1985 Aug 10	90	RCA
I	1985 Aug 10	90	RCA

The treatment of the images, as described in previous papers, involved several steps: (1) the determinations of the sky level using both an iterative procedure and offset frames; (2) the localization of the cluster center by means of the "mirror autocorrelation" method (see Djorgovski 1988); (3) the determination of a modal background used as a reference level for the definition of the apparent extinctions; and, finally, (4) the identification of the dust cloud candidates.

It must be pointed out that since the extinction is measured in a differential way, the existence of dust along the line of sight to the cluster should not affect the results, provided that this material behaves in a uniform way on scale lengths of some tens of arcseconds.

2.2. *Polarimetry*

Unfiltered polarimetry was obtained for a number of stars distributed in the field of the cluster as well as for its nucleus.

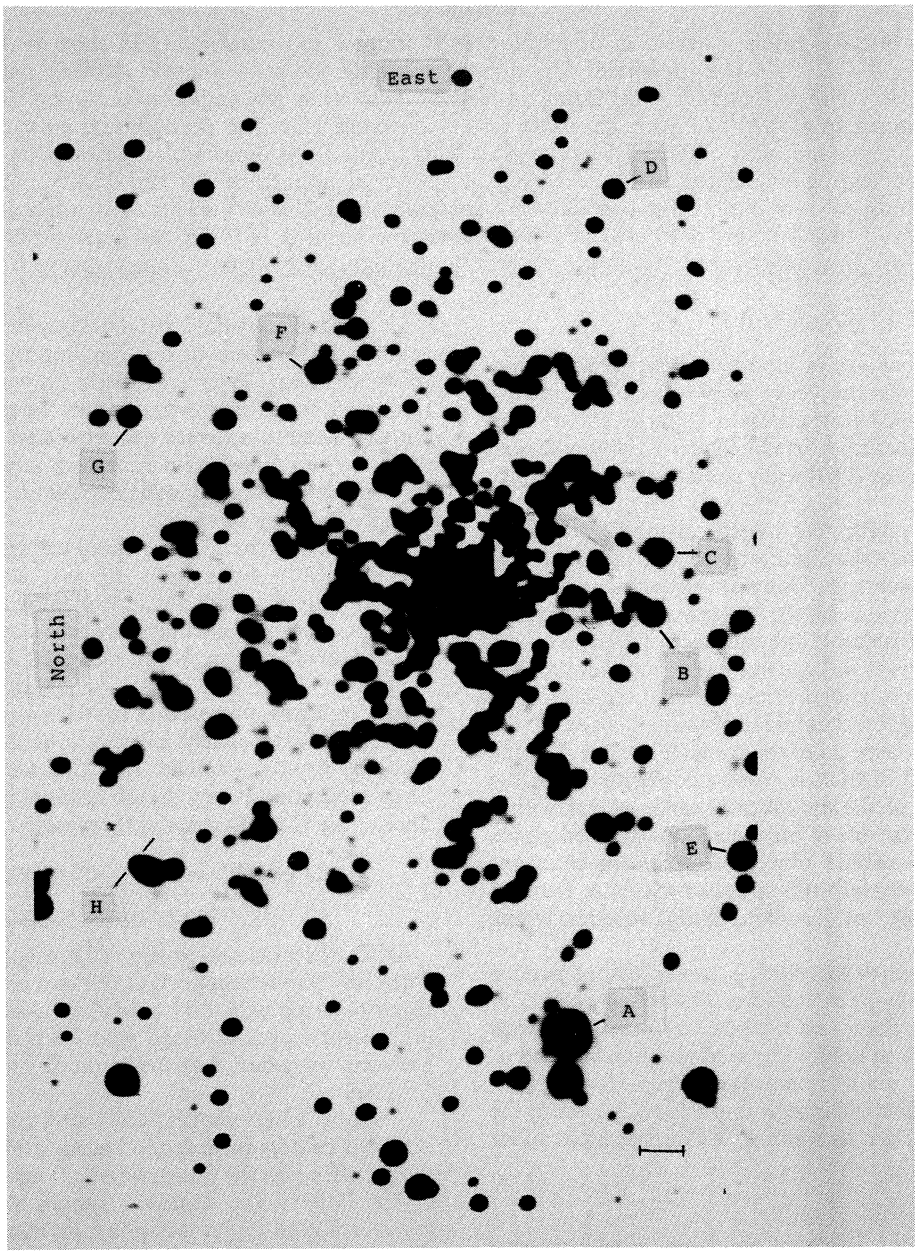

FIG. 1.—Background-subtracted visual image of NGC 6624. Letters identify stars listed in Table 2. The horizontal bar (*lower right*) is 10″ long. North is to the left, and east is up.

TABLE 2

UNFILTERED POLARIMETRY

Star	X	Y	P(%)	εP	P.A.	Comment[a]
A	220	74	1.43	0.05	111°.8	
B	253	257	1.33	0.09	114.3	III-2
C	258	284	1.37	0.08	111.2	
D	237	441	1.29	0.11	109.6	II-111
E	295	151	1.36	0.08	111.6	III-125
F	116	360	1.30	0.08	110.8	I-26
G	38	340	1.41	0.16	112.6	
H	44	146	1.21	0.07	110	
Average			1.34	0.07	111.4	
Nucleus	174	275	1.36	0.05	113.3	

[a] Identifications from Liller & Carney 1978.

These observations were carried out by means of the Vatpol polarimeter attached to the 215 cm telescope at the Complejo Astronómico "El Leoncito" and using an S-20 photocathode.

Both zero polarization and standard stars were observed during the run. The observations, made through a 5″ diaphragm, are given in Table 2 where the stars are numbered according to their identifications in Figure 1. The rectangular coordinates (in pixel units) are defined in a system with the x- and y-axes pointing toward the south and east, respectively.

In this system, the cluster nucleus is at $x = 174$, $y = 275$.

3. THE SMOOTH BACKGROUND AND THE FOREGROUND EXTINCTION

As in previous papers (e.g., FM), the reference modal background was determined by computing the mode of the pixel intensity distribution within rings concentric with the cluster nuleus.

In order to minimize the possible effect of foreground or intracluster extinction on this reference level, a modal profile was obtained in each quadrant ranging from 12″ to 90″ from the cluster center. The central region was avoided because the overlapping of the seeing profiles of the brightest stars precludes the sampling of the underlying background.

The modal profiles in the four different quadrants were then overlapped and the upper envelope was adopted as representative of the overall cluster background. A least-squares fit to these values, shown in Figure 2, yield (in mag arcsec^{-2})

$$\mu_V = 4.02 \log (r/r_c) + 17.48 \quad 12'' \leq r \leq 22''$$

$$\mu_V = 5.02 \log (r/r_c) + 17.28 \quad r > 22'' .$$

In these approximations we adopted $r_c = 12''.5$ because, in the fitting range, the mean profiles are consistent with a King (1962) analytical profile with the core radius and a large r_t/r_c ratio.

To within the errors, no differences were found in the slopes corresponding to the different filters, implying no radial color gradients. The resulting colors for the modal background are

$$(U-B) = 0.31 \pm 0.06 ,$$

$$(B-V) = 0.82 \pm 0.04 ,$$

$$(V-R) = 0.063 \pm 0.05 ,$$

$$(V-I) = 1.27 \pm 0.04 .$$

In order to test the reliability of the derived modal profile, and for statistical purposes discussed in a following paragraph,

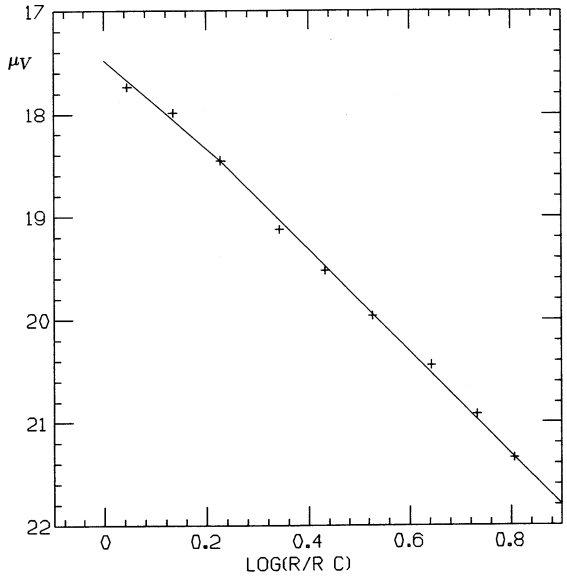

FIG. 2.—Modal visual surface brightness for NGC 6624. The straight lines represent the adopted background as defined in the text. The adopted value for r_c is 12″.5.

we constructed an artificial tridimensional cluster used to simulate a CCD frame, including seeing and read-out noise effects.

The stars were spatially distributed according to a density law

$$\rho = \rho o/[1 + (r/r_c)^2]^{3/2} ,$$

which is appropriate for a cluster with a very large tidal radius. The apparent magnitudes were generated following a 47 Tuc luminosity function, a fact that is justified by the morphology of the giant branches in both clusters, and also by the similitude (within ±0.02 mag) of their integrated intrinsic colors (see Reed, Hesser, & Shawl 1987). Since NGC 6624 has some 400 stars brighter than $V = 17.7$, in an annular region defined between 12″ and 75″, the adopted luminosity function leads to a total number of 58,000 stars brighter than $V = 25$ for the whole cluster (inside $6r_c$).

The spatial position of these model stars was projected on the sky plane and their brightness was convolved with a point-spread function similar to that of the visual frame. Finally, Gaussian noise was added to simulate read-out effects. The resulting modal background obtained for the simulated cluster is depicted in Figure 3 where the solid line is the fit obtained for the observed profile. This figure shows that the model cluster matches the observed background, with maximum deviations smaller than 0.1 mag.

The behavior of the foreground extinction can be tested by means of integrated photometry and also using the polarimetric observations. Table 3 gives the integrated V brightness in the four different quadrants (in annular segments with internal and external radii of 12″.5 and 75″, respectively). These values have an average of $V = 10.11$ with a rms of 0.03 mag, and indicate the absence of an *overall gradient* in the foreground extinction across the cluster field. A similar conclusion can be obtained from the behavior of the polarization of individual stars, depicted as a function of the angular distance to the cluster center in Figure 4. It must be noted, however, that the bulk of the polarization arises in dust close to the Galactic

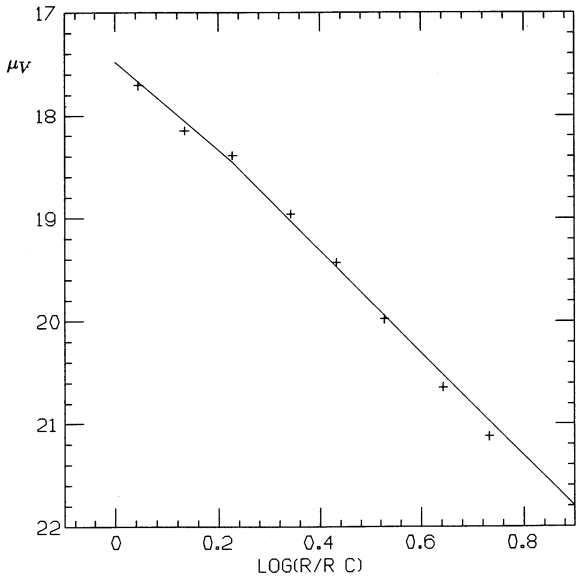

FIG. 3.—Modal visual surface brightness for an artificial globular cluster matching the NGC 6624 photometric parameters. The straight lines are the same shown in Fig. 2.

plane and aligned by the local magnetic field. Dust, located far from the plane (NGC 6624 lies at some 1.1 kpc), and with nonaligned grains, might be present without contributing to the observed polarization.

The integrated colors of the cluster and those of the modal background are depicted in Figure 5. The arrows indicate the dereddened positions adopting the color excess $E(B-V) = 0.28$, and color excess ratios given in Reed et al. (1987). The intrinsic colors of the background agree, to within the errors, with those of the integrated main sequence of 47 Tuc, thus indicating that most of the light arises in main-sequence stars. In turn, this fact agrees with the analysis of the model cluster, where 60% of the V light comes from dwarf stars.

4. APPARENT EXTINCTIONS

Using the visual frame, a new image was created with pixels defined as

$$a_V = (I - I_s)/(I_m - I_s) ,$$

where I is the observed visual intensity at each pixel, and I_m, I_s are the modal and sky levels, respectively. All contiguous N_p pixels with a_V smaller than 0.76 were used to define a mask and compute the average extinction:

$$A_\lambda = -2.5 \log (a_\lambda)$$

for each patch on the different color frames.

TABLE 3

INTEGRATED V PHOTOMETRY

Aperture	V Magnitude	Comments[a]
25″	10.05	10.03
137	8.41	8.50
NE 12.5–75	10.16	
NW 12.5–75	10.12	
SE 12.5—75	10.09	
SW 12.5–75	10.07	

[a] Comparison values from van den Bergh 1977.

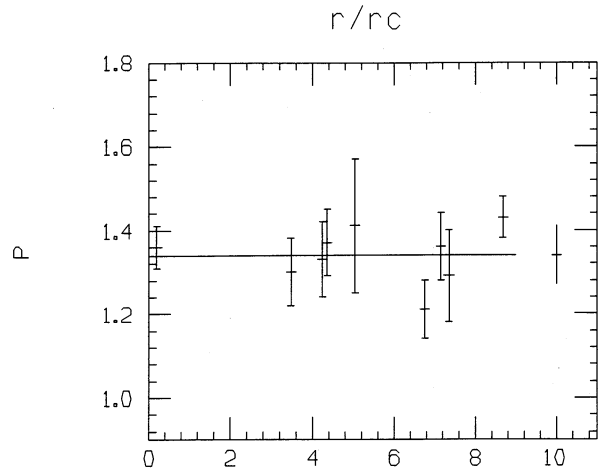

FIG. 4.—Polarization values for stars listed in Table 2 as a function of the distance to the cluster center. The horizontal line is the average value. The values at the extreme left and right are those corresponding to the cluster nucleus and the rms of the stellar polarizations respectively.

The adoption of $a_V = 0.76$, which corresponds to a brightness level 0.30 mag below the modal background, to define a patch helps to reject mere statistical fluctuations but also introduces a selective effect against the detection of low optical depth clouds.

The effect of the uncertainties in the values of I_m and I_s on the derived extinctions was estimated as ± 0.07 to ± 0.12 mag for patches at $r/r_c = 1.0$ and 3.5, respectively.

The rectangular positions of all the measured patches, as well as their pseudoradius defined as $r = (N_p/\pi)^{1/2}$ and average apparent extinctions, are listed in Table 4. The rms values, also given in this table, were computed including all the pixels within the contour of a given patch as defined by the mask image.

Table 4 shows that most patches (but not all) have a "gray" behavior indicating that the sampling is in fact dominated by statistical "holes." Further analysis requires the discussion of

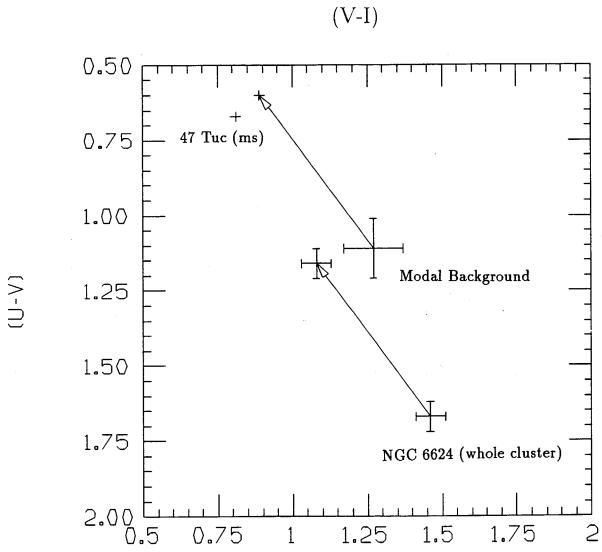

FIG. 5.—Integrated colors for the whole cluster and modal background. The arrows indicate the dereddened colors. The small cross represents the intrinsic integrated colors of the 47 Tuc main sequence.

TABLE 4

APPARENT EXTINCTIONS FOR DARK PATCHES

N	r/r_c	x	y	r*	A_U (mag)	σ_U	A_B (mag)	σ_B	A_V (mag)	σ_V	A_R (mag)	σ_R	A_I (mag)	σ_I
1.....	4.0	86	215	2.26	0.38	8	0.45	10	0.32	3	0.37	4	0.24	6
2.....	3.4	85	269	4.11	0.48	16	0.44	14	0.43	11	0.44	11	0.38	12
3.....	3.1	95	271	5.05	0.42	15	0.46	13	0.47	11	0.46	11	0.46	11
4.....	4.2	91	337	3.74	0.32	9	0.26	8	0.40	9	0.37	13	0.29	13
5.....	3.4	102	321	1.87	0.34	11	0.40	12	0.43	5	0.33	5	0.30	8
6.....	3.3	115	331	3.66	0.33	10	0.39	11	0.38	11	0.36	9	0.30	9
7.....	2.3	114	266	3.24	0.40	8	0.42	9	0.37	8	0.38	8	0.41	7
8.....	2.6	117	234	2.71	0.38	8	0.35	9	0.36	8	0.34	11	0.37	11
9.....	2.8	120	222	1.78	0.38	4	0.29	3	0.33	5	0.32	5	0.36	5
10.....	2.2	124	242	3.29	0.38	11	0.41	8	0.39	8	0.48	10	0.47	8
11.....	2.7	120	314	2.46	0.29	8	0.30	9	0.40	9	0.40	12	0.36	8
12.....	2.8	124	323	3.29	0.29	12	0.34	9	0.35	7	0.35	9	0.26	13
13.....	3.1	125	209	2.93	0.47	9	0.32	8	0.32	4	0.30	6	0.30	6
14.....	3.5	135	351	5.32	0.46	18	0.57	18	0.51	15	0.46	18	0.33	16
15.....	2.1	147	223	2.26	0.24	8	0.27	6	0.31	3	0.33	6	0.32	5
16.....	3.1	147	195	2.46	0.48	13	0.33	11	0.32	3	0.28	6	0.21	5
17.....	1.9	142	234	3.19	0.42	14	0.38	8	0.37	8	0.37	9	0.35	12
18.....	1.9	164	222	4.92	0.42	13	0.43	9	0.39	9	0.41	9	0.38	10
19.....	1.5	167	233	4.33	0.39	9	0.40	5	0.39	7	0.41	8	0.40	7
20.....	2.8	167	200	2.70	0.38	10	0.27	9	0.28	10	0.25	10	0.10	10
21.....	1.8	170	225	5.14	0.38	10	0.41	7	0.38	8	0.41	7	0.38	9
22.....	2.3	174	212	2.71	0.37	6	0.39	4	0.33	5	0.38	6	0.34	6
23.....	2.0	190	318	4.89	0.44	9	0.45	9	0.42	10	0.43	10	0.43	9
24.....	2.9	197	200	1.78	0.34	5	0.38	3	0.32	3	0.27	2	0.17	4
25.....	2.6	202	329	2.99	0.55	8	0.45	9	0.33	4	0.30	7	0.30	7
26.....	1.5	204	249	5.41	0.60	11	0.50	12	0.44	13	0.40	12	0.31	14
27.....	3.3	210	343	2.88	0.42	10	0.42	13	0.35	8	0.34	8	0.25	7
28.....	2.3	215	233	4.22	0.41	9	0.40	7	0.39	6	0.39	6	0.41	6
29.....	2.0	222	272	2.76	0.62	8	0.44	7	0.39	7	0.38	7	0.39	8
30.....	2.1	223	288	4.15	0.42	8	0.36	6	0.33	4	0.31	5	0.33	5
31.....	3.3	227	209	3.14	0.28	13	0.35	9	0.35	5	0.33	6	0.40	9
32.....	3.0	232	223	2.71	0.36	6	0.38	10	0.36	6	0.33	11	0.38	8
33.....	2.7	235	244	2.46	0.39	6	0.32	5	0.32	4	0.37	6	0.42	7
34.....	2.7	240	277	1.95	0.43	4	0.36	8	0.33	4	0.31	8	0.36	7
35.....	3.6	245	2.17	4.33	0.39	7	0.41	12	0.40	9	0.42	11	0.49	13
36.....	4.3	250	347	3.39	...	...	0.37	10	0.36	6	0.36	10	0.31	10
37.....	4.1	252	337	4.79	0.53	17	0.42	13	0.38	11	0.44	16	0.33	14
38.....	3.6	257	299	3.29	0.53	8	0.32	7	0.33	3	0.29	8	0.23	10
39.....	3.4	257	269	2.71	0.42	8	0.34	11	0.32	3	0.17	6	0.11	7
40.....	4.1	270	299	3.04	0.22	9	0.33	8	0.36	6	0.32	9	0.24	8
41.....	4.3	272	230	3.24	0.17	13	0.25	14	0.33	5	0.30	13	0.41	14
42.....	4.1	272	247	3.04	0.49	14	0.44	15	0.40	9	0.42	18	0.42	20
43.....	3.9	94	329	3.30	0.36	4	0.29	10	0.37	7	0.34	9	0.33	13
44.....	1.8	134	294	4.18	0.33	7	0.37	6	0.33	5	0.38	7	0.41	8
45.....	2.1	162	321	3.43	0.38	10	0.39	7	0.34	5	0.36	4	0.31	3
46.....	2.6	147	331	2.52	0.33	7	0.36	4	0.31	3	0.30	4	0.15	6
47.....	2.4	154	329	2.76	0.30	8	0.36	5	0.31	3	0.31	6	0.22	8
48.....	3.2	222	334	2.93	0.36	8	0.36	10	0.33	5	0.31	7	0.29	9
49.....	2.5	167	332	1.00	0.31	10	0.29	11	0.28	11	0.32	8	0.28	10

NOTE.—Extinctions in magnitudes; rms values in hundredths of a magnitude.

the photometric behavior for a cloud embedded in a globular cluster.

A preliminary approach to model the apparent extinction of a cloud with optical τ inside a globular cluster was included in previous papers (e.g., FM). A more complete description can be given with

$$A_\lambda = -2.5 \log [l\alpha + (1 - l)e^{-\tau}\alpha + S_{\lambda n} + S_{\lambda i}] ,$$

where l is the column brightness in front of the cloud, in terms of the modal brightness along the line of sight; α is a measure of the deviation of the real local background from the overall value defined for a given angular distance to the cluster center; and $S_{\lambda n}$, $S_{\lambda i}$ are the nebular and instrumental contributions to the scattered light.

Modeling the photometric behavior of a dust cloud in terms of this last expression needs a number of assumptions which are not completely justified. For example, the characteristics of dust associated with a Population II environment are not known. In what follows, however, we adopt a value of the selective extinction ratio $R = 3.5$ which is appropriate for a background with integrated spectral type G2, and color excess slopes $E(U-B)/E(B-V) = 0.83$, $E(V-I)/E(B-V) = 1.35$ (Reed et al. 1987) derived from globular clusters reddened by "normal" interstellar dust.

Models containing all the described ingredients (Forte, Mendez, & Bassino 1992) show that clouds with a wide range of intrinsic optical depths might, under given circumstances, have very similar apparent extinction curves.

As a consequence of this fact, we adopted a conservative hypothesis: The dust clouds have small optical depths

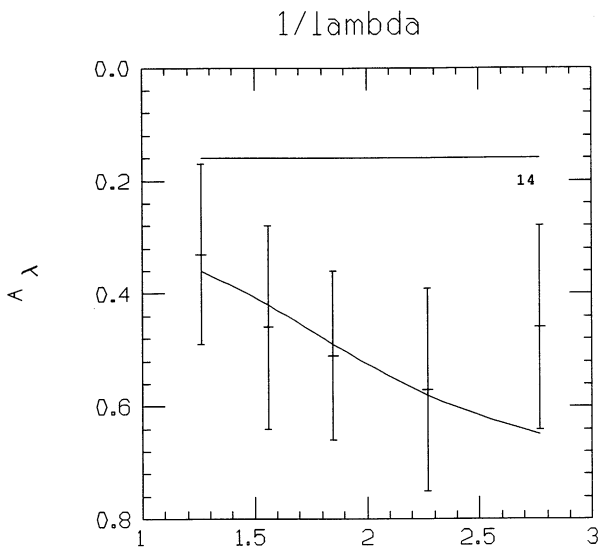

FIG. 6*a*

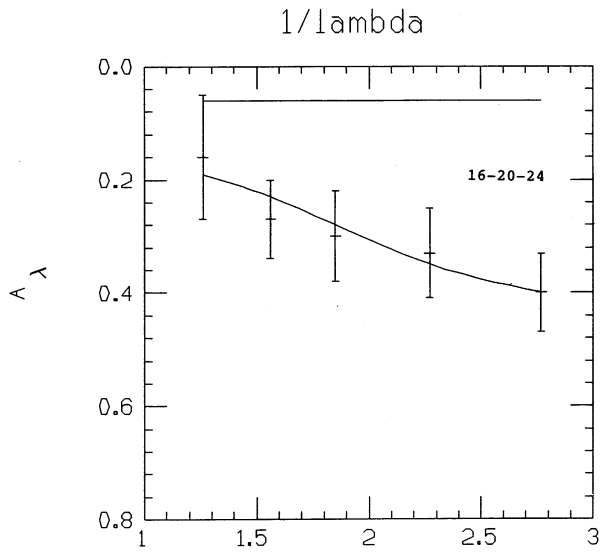

FIG. 6*b*

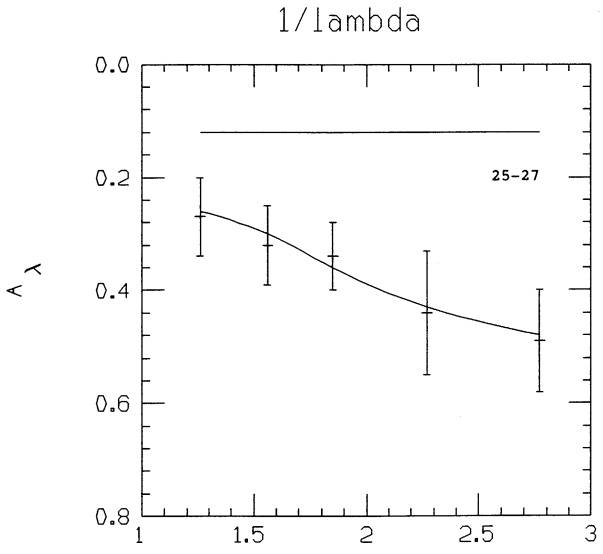

FIG. 6*c*

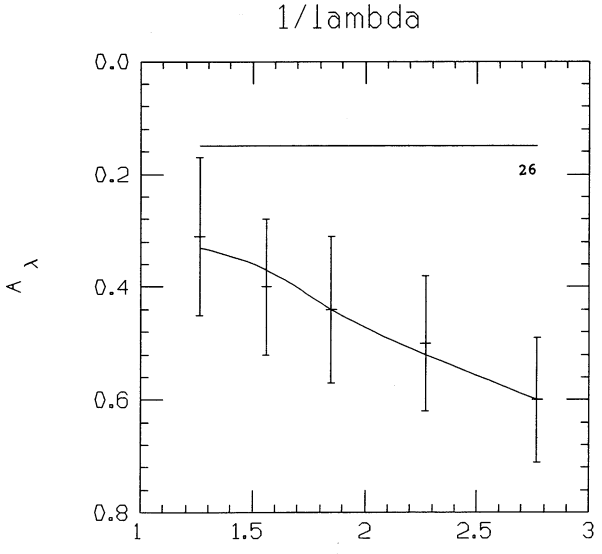

FIG. 6*d*

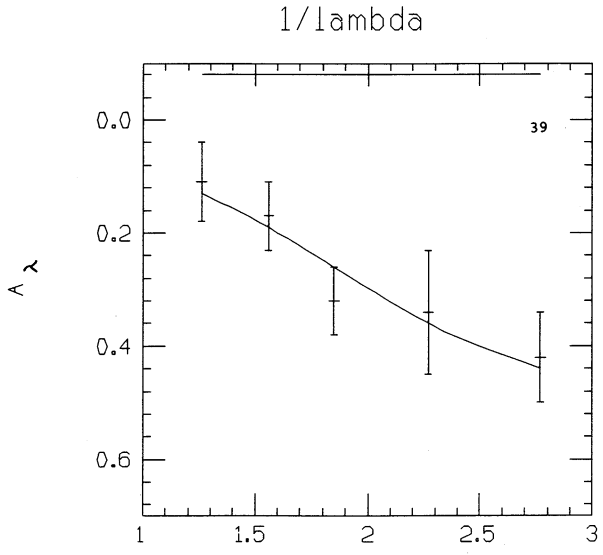

FIG. 6*e*

FIG. 6.—Selective extinction fits for dust cloud-candidates listed in Table 5. The vertical bars represent the rms values of the averages at each wavelength. The horizontal line is the position of the local background Δ. Extinctions are given in magnitudes and the wavelengths in microns.

(implying low scattering effects) and are located at low l values where they can be more easily detected. Then,

$$A_\lambda = -2.5 \log (e^{-\tau}\alpha)$$

and if background fluctuations α have a gray behavior,

$$A_\lambda = A_\lambda^* + \Delta$$

where A_λ^* is the minimum optical depth that, seen against a background offset Δ, will match the observed wavelength behavior of the apparent extinctions. Under these assumptions, and adopting selective extinction coefficients compatible with the adopted R value, the minimum intrinsic visual extinctions can be found using:

$$A_I = 0.61A_V^* + \Delta ,$$
$$A_R = 0.77A_V^* + \Delta ,$$
$$A_V = 1.00A_V^* + \Delta ,$$
$$A_B = 1.28A_V^* + \Delta ,$$
$$A_U = 1.51A_V^* + \Delta .$$

These expressions show that "large" apparent extinctions and low color amplitude variations do not necessarily require high l and optical depths as assumed in previous papers (e.g., FM).

The slopes A_λ^* and standard error of the regression σ were computed for all patches listed in Table 4, as well as the ratio $t = A_V^*/\sigma$. In 41 cases, the slopes were close to zero and had t values smaller than 1, indicating that they are mostly gray background fluctuations. In turn, seven patches exhibited detectable slopes with t larger than 2 and up to 7.2, namely, patches 16, 20, 24, 25, 26, 27, and 39. Since the dark patches 16, 20, 24 and 25, 27, lie spatially close to each other, they were combined in two single patches. The resulting minimum visual extinctions, errors of the regression, gray offsets Δ, sampled areas, and t ratios are given in Table 5. The effect of instrumental scattering was estimated by mapping the position of the stars brighter than $V = 16.0$ in the immediate neighborhood of each patch and using the point-spread function of each frame. In all cases, and for the five filters, the maximum effect on the apparent extinctions was smaller than 0.03 mag, and no explicit correction was added to the derived values.

For the cloud candidates we tested the "null hypothesis" that the A_V^* are zero. Using a 5% significance level, a 3 degree of freedom fit, and tables from Crow, Davis, & Maxfield (1972), we find that this hypothesis can be rejected in all cases. The 90% confidence intervals for the derived minimum intrinsic visual extinctions ΔA_V^* are also given in Table 5.

The selective extinction curve fittings for the dust cloud candidates are depicted in Figure 6, where the vertical bars represent the rms of the averages. Patch 14 is also included as a dubious case since $BVRI$ extinctions seem to indicate differential extinction, although the U value lies well above the fit made through the other filters.

TABLE 5

EXTINCTION PARAMETERS FOR DUST CLOUD CANDIDATES

N	A_V^* σ	Δ	Area (pixels)	t	ΔA_V^*
14[a]	0.33 ± 0.05	0.16	88	4.2	±0.10
16, 20, 24	0.23 ± 0.07	0.06	86	3.1	±0.16
25, 27	0.24 ± 0.03	0.12	55	7.3	±0.07
26	0.29 ± 0.04	0.15	92	7.4	±0.09
39	0.34 ± 0.06	−0.08	36	5.9	±0.14

[a] Without considering the U value.

5. THE DISTRIBUTION AND OPTICAL DEPTH OF THE DUST CLOUD CANDIDATES

Figure 7 (Plate 5) shows the visual frame, before and after subtracting the modal background, indicating the position of the dust cloud candidates. An inspection of this figure reveals that the dark patches are not evenly distributed, as expected in the case of random fluctuations enhanced by the subtraction of the background.

A quantitative description on this situation can be made, for example, dividing the image in northern and southern halves, counting the number of pixels, with a given fractional brightness F, in annular segments and computing the differences ΔN. These differences should be, in the case of random fluctuations, close to zero. However, these quantities have a strong systematic behavior as shown in Figure 8*a* where the differences have been computed for annular segments with $1r_c$ widths (from 1 to $6r_c$) and denote that the cluster center is not the barycenter of the dark patch distribution. Alternatively, this strong asymmetry is not detectable in the east–west direction as seen in Figure 8*b*.

Most of the dark patches and cloud candidates seem to lie within a 50″ radius circle centered at $x = 195$, $y = 292$. The southern segment of this circle coincides with a dark arc spanning almost 180°. This arc is not an artifact of the background subtraction procedure, and its existence, as described in what follows, is also supported by a photometric analysis of the raw image.

Table 6 gives the average modal brightness for annular segments in the four different quadrants. The comparison of these values reveals that the southern quadrants are some 0.2 mag fainter than their northern counterparts between 4 and $5r_c$. The situation is reversed for the innermost annular segment and the overall geometry can be described as a somewhat flattened ring or bubble seen in projection on the cluster contour. These deviations are larger than the expected statistical fluctuations, derived from the artificial cluster described in § 3 and listed in the last column of Table 6, and thus are attributable to differential extinction.

It can be noted that this differential extinction agrees with the range of minimum intrinsic extinctions obtained from the color analysis of the dust cloud candidates.

The arguments presented in the previous paragraph and those discussed in this section are then consistent in the sense

TABLE 6

MODAL SURFACE BRIGHTNESS IN ANNULAR SEGMENTS[a]

	N		S			
r/r_c	E	W	E	W	DIFFERENCE[b] N–S	σ[c] Model
1–2.....	18.40	18.58	18.26	18.29	+0.21	0.12
2–3.....	19.37	19.39	19.36	19.36	+0.02	0.11
3–4.....	20.04	19.96	19.98	20.12	−0.05	0.09
4–5.....	20.40	20.46	20.67	20.64	−0.22	0.05
5–6.....	21.00	20.93	20.93	20.99	−0.04	0.05

[a] In mag arcsec^{-2}.
[b] Average difference N–S.
[c] rms values of the N–S differences from the model cluster.

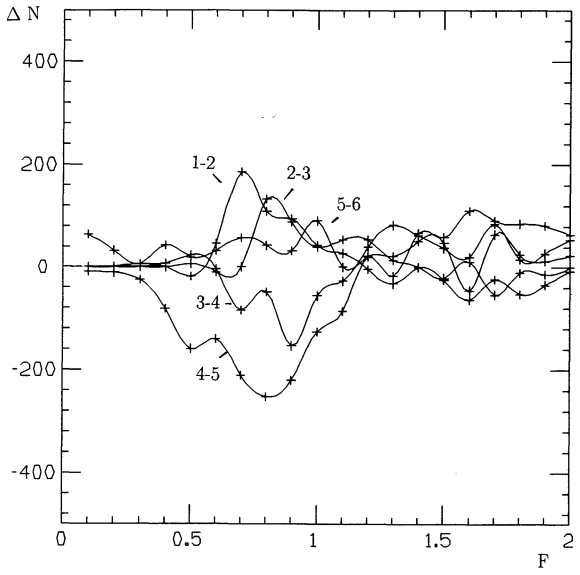

FIG. 8a

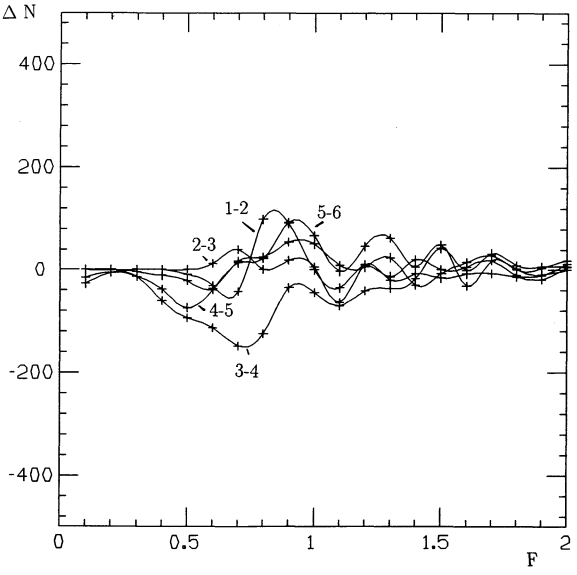

FIG. 8b

FIG. 8.—(*a*) Distribution of the pixel count differences (for pixels with a given fractional brightness *F*) in five northern and southern semirings (starting with $r/r_c = 1$ and widths equal to $1r_c$). *F* is defined by normalizing the pixel brightness with the value of the modal background fit at the pixel position. (*b*) Same as (*a*) but for eastern and western rings.

that there is an optically thin dust component producing differential extinction and with a large-scale geometry. The question that now remains open is if this dust is just along the line of sight and between the Galactic plane dust layer and NGC 6624 or associated with the cluster itself.

An answer to this question can be obtained from the analysis of the color-magnitude diagram published by Liller & Carney (1978). Figure 9 shows a *V* versus $(B-V)$ diagram for all the stars measured by these authors in an annular region between 35″ and 75″ from the cluster center. No differences are detectable in the appearance of the color-magnitude diagrams when the stars are discriminated according to their positions in the different quadrants except for the SE one, where the effect of the dark arc is more evident. Five stars in this quadrant appear clearly shifted from the average position of the remaining stars, suggesting differential reddening. Alternatively, it might be argued that these objects are merely field interlopers (i.e., nonmembers). However, the fact that they appear only in the SE quadrant and on the isophotal deformation of the cluster strongly suggest that it is not the case.

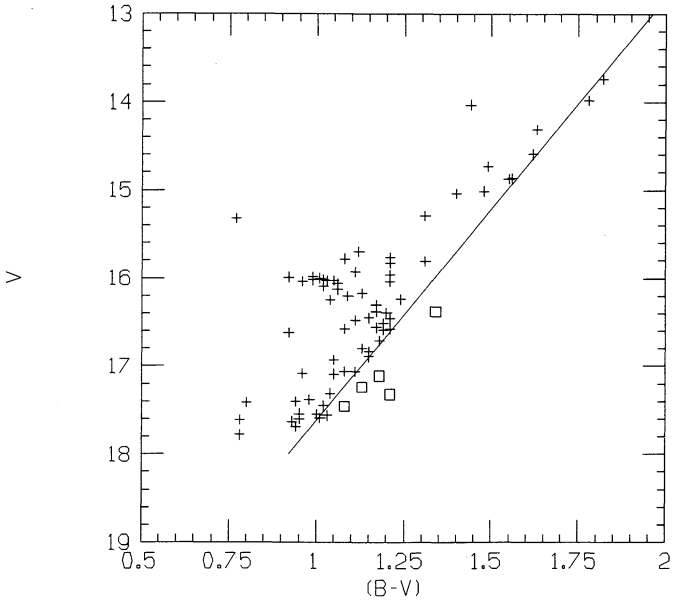

FIG. 9.—Color-magnitude diagram for NGC 6624 stars (values from Liller & Carney 1978) inside $6r_c$. Squares are stars located in the dark arc mentioned in the text. The solid line used as a reference for measuring the differential extinctions, as explained in the text, is also shown.

An estimate of the differential extinction on these stars was obtained by defining the mean position of the giant branch as

$$V = -4.63(B-V) + 22.03 .$$

This line corresponds to a giant branch "height" $\Delta V_{1.4} = 1.75$ which is consistent with the cluster metallicity (Zinn & West 1984). The differential extinctions were then obtained by shifting the observed *V* and $(B-V)$ values along lines with a slope $R = 3.5$ toward the interception with the mean position of the giant sequence and are listed in Table 7. It must be noted that these stars appear spatially mixed (on the sky) with other stars that, spanning the same brightness range, exhibit the average color magnitude behavior of the cluster (e.g., II-5, II-30, II-31, II-32, II-38, III-9, III-9, III-18). This situation is conceivable if the dust producing the differential extinction is located within the cluster.

TABLE 7

DIFFERENTIAL EXTINCTION FOR STARS IN NGC 6624

Star	*V* (mag)	$(B-V)$ (mag)	ΔA_V (mag)
II-13	16.38	1.34	0.24
II-37	17.11	1.18	0.24
II-42	17.32	1.21	0.39
II-49	17.24	1.13	0.20
II-50	17.46	1.08	0.21
Average			0.26 ± 0.08

Furthermore, the range of differential extinctions given in Table 7 is comparable with the values obtained from the dark patches color analysis and from the differential photometry.

The total dust mass is difficult to estimate because the apparent sizes of the individual dark patches are limited, mainly by the star-to-star separations and their seeing profiles. A crude value can be obtained by assuming that the dust feature can be approximated as two half-ring segments with inner and outer radii of 12".5 and 25" (for the innermost segment) and 100" and 125", respectively, and adopting a mean optical depth of 0.25 mag. This approximation leads to masses ranging from 0.07–0.8 $M_\odot$, if the adopted grain composition is graphite or silicate-like, respectively.

6. DISCUSSION

Independent arguments based on the color analysis of a number of dark patches, and modal photometry suggest the presence of a large dust feature producing differential extinction (on top of the relatively uniform foreground component) within a circle 100" in diameter not centered on the NGC 6624 nucleus. The optical depths derived with both methods, in turn, are consistent with the position of some stars in the color-magnitude diagram. The photometric behavior of these stars, and others located in the same field, strongly suggests that the dust producing differential extinction is located within the cluster.

The appearance of the dark patch distribution is strongly asymmetric (i.e., not centered at the cluster nucleus) and show an arc or ringlike pattern. The tridimensional shape of the dust responsible for this geometry canot be unambiguously determined, but it is compatible with a bubble or shell with a 2–2.5 pc radius seen in projection against the plane of the sky.

The estimated mass is largely uncertain but not inconsistent with the upper limit derived from 100 μm *IRAS* flux discussed by Lynch & Rossano (1990). We note that these authors adopt a very high dust equilibrium temperature (50° K) which, at the outer region of a globular cluster, may be substantially lower (see, for example, Gillett et al. 1988). An equilibrium temperature close to 20° would raise their value to some 0.3 $M_\odot$.

The origin of such a kind of structure is not clear. However, it can be mentioned that dust shells with scale sizes of one to several parsecs, and low optical depths, can be detected around some red giant stars (e.g., Gillett et al. 1986; Hawkins 1990). Pre–planetary nebula objects are also good candidates as possible dust sources within globular clusters (Gillett et al. 1989). Alternatively, some novae, as GK Per, appear clearly associated with dusty structures (Seaquist et al. 1989) of a similar size.

If a dust structure of this type is expanding at the typical velocities quoted for shells ejected from red giants or pre–planetary nebula objects (e.g., 30 km s^{-1}), which in turn are comparable to the cluster escape velocity (27 km s^{-1}; Webbink 1981), its size would imply a time scale of some 3×10^5 yr. This relatively ephimeral duration would conspire against the detection of a large number of shells in other clusters. In this frame, however, the relatively isolated dark patches seen in other clusters might be the remnants of similar but older events.

A search for a possible progenitor star, carried out in the neighborhood of the barycenter of the dark patches, did not yield a clear candidate. However, the spatial coincidence between the apparent barycenter of the dark patch distribution and the reported position of the very short period burster 1820−30 (Baylin et al. 1988) remains as an intriguing subject. Furthermore, this fact, and the tentative detection of a rapidly expanding nebula (Bel et al. 1980) in the same area, would certainly deserve further investigations.

REFERENCES

Aurière, M., & Leroy, J. L. 1990, A&A, 234, 164
Baylin, Ch. D., Grindlay, J. E., Cohn, H., & Lugger, P. M. 1988, ApJ, 331, 303
Bel, N., Clavel, J., & Foy, R. 1980, in Second *IUE* Conference (ESA SP-157), 183
Crow, E. L., Davis, F. A., & Maxfield, M. W., ed. 1972, Statistics Manual (New York: Dover)
Djorgovski, S. 1988, in IAU Symp. 126, Globular Clusters in Galaxies, ed. J. Grindlay & A. G. D. Phillip (Dordrecht: Reidel), 333
Forte, J. C., & Méndez, M. 1987, AJ, 95, 500 (FM)
———. 1989, ApJ, 345, 222
Forte, J. C., Mendez, M., & Bassino, L. 1992, in preparation
Gillett, F. C., Backman, D. E., Beichman, C., & Neugebauer, G. 1986, ApJ, 310, 842
Gillett, F. C., De Jong, T., Neugebauer, G., Rice, W. L., & Emerson, J. P. 1988, AJ, 96, 116
Gillett, F. C., Jacoby, G. H., Joyce, R. R., Cohen, J. G., Neugebauer, G., Soifer, B. T., Nakajima, T., & Matthews, K. 1989, ApJ, 338, 862
Hawkins, G. W. 1990, A&A, 229, L5
King, I. R. 1962, AJ, 67, 471
Liller, M., & Carney, B. W. 1978, ApJ, 224, 383
Lynch, D. K., & Rossano, G. S. 1990, AJ, 100, 719
Méndez, M., Forte, J. C., & Orsatti, A. M. 1989, ApJ, 338, 136
Reed, B. C., Hesser, J. E., & Shawl, S. J. 1987, PASP, 100, 545
Rosse, Earle of, 1861, Phil. Trans. R. Soc. Lond., 151, plate 28
Scott, E. H., & Durisen, R. H. 1978, ApJ, 222, 612
Seaquist, E. R., Bode, M. F., Frail, D. A., Roberts, J. A., Evans, A., & Albinson, J. S. 1989, ApJ, 344, 805
Vandenberg, D. 1978, ApJ, 224, 394
van den Bergh, S. 1977, AJ, 82, 796
Webbink, R. F. 1981, ApJS, 45, 259
Zinn, R., & West, M. J. 1984, ApJS, 55, 45

1992ApJ...388..383F

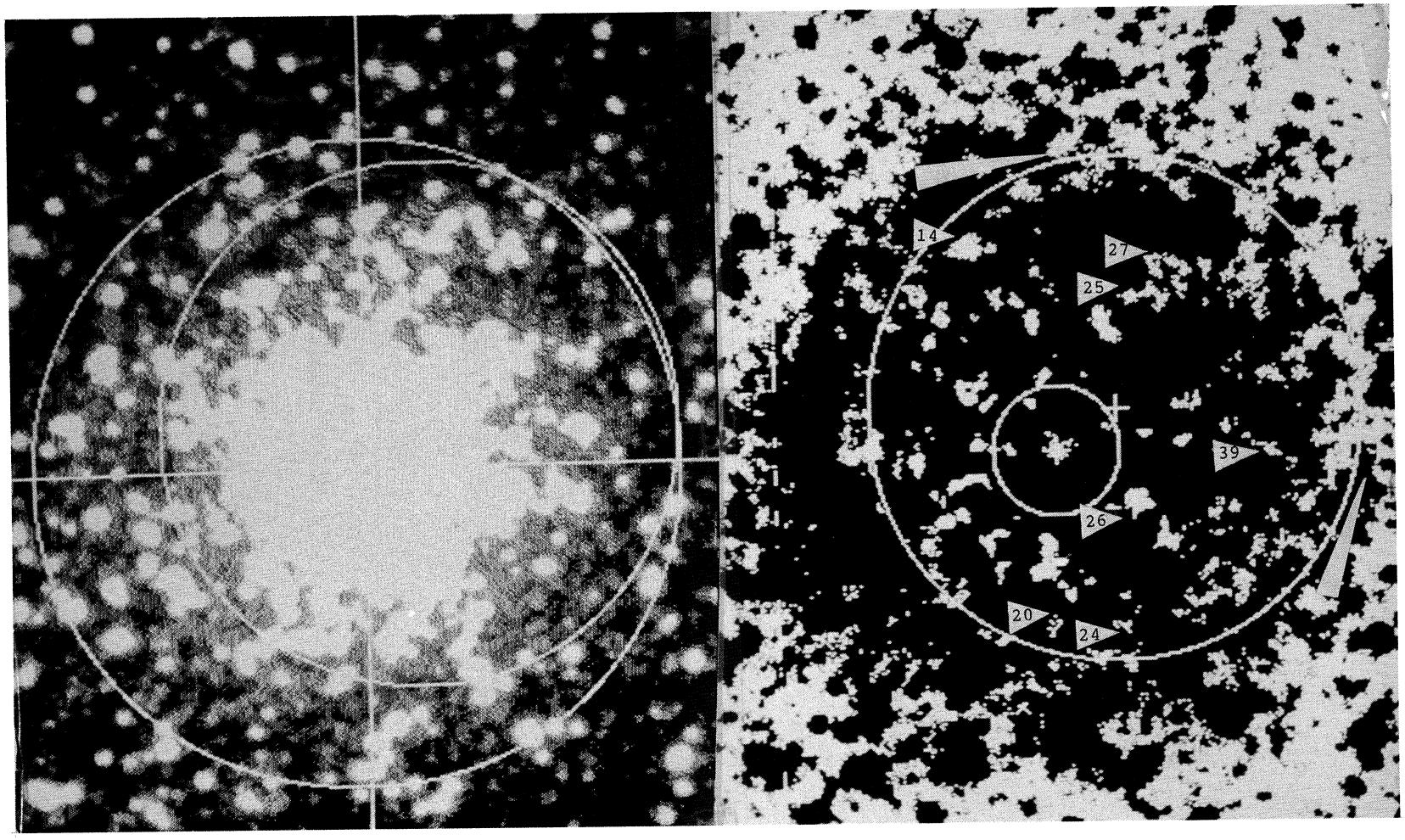

FIG. 7*a*

FIG. 7*b*

FIG. 7.—(*a*) Visual CCD image of NGC 6624. North is to the left, and east is up. The large circle has a 62″.5 radius ($5r_c$) and is centered at the cluster nucleus (the interception of the straight lines). The small circle has a 50″ radius and is centered on a tentative barycenter of the dark patch distribution. (*b*) Composite image showing the distribution of the (enhanced) dark patches and dust cloud candidates. The 50″ circle centered at the barycenter of the dark patch distribution is also shown. The small circle has a $1r_c$ radius. The white arrows point to the dark arc mentioned in the text.